ELSEVIER

Contents lists available at ScienceDirect

Toxicology and Applied Pharmacology

journal homepage: www.elsevier.com/locate/taap



Doxorubicin obliterates mouse ovarian reserve through both primordial follicle atresia and overactivation



Yingzheng Wang^a, Mingjun Liu^a, Sarah B. Johnson^a, Gehui Yuan^{a,b}, Alana K. Arriba^a, Maria E. Zubizarreta^a, Saurabh Chatterjee^a, Mitzi Nagarkatti^c, Prakash Nagarkatti^c, Shuo Xiao^{a,*}

- ^a Department of Environmental Health Sciences, Arnold School of Public Health, University of South Carolina, Columbia, SC 29208, USA
- b Department of Hygienic Analysis and Detection, School of Public Health, Nanjing Medical University, Nanjing 21009, China
- ^c Department of Microbiology and Immunology, School of Medicine, University of South Carolina, SC 29208, USA

ARTICLE INFO

Keywords: Chemotherapy Doxorubicin Primordial follicle Ovarian reserve Fertility

ABSTRACT

Ovarian toxicity and infertility are major side effects of cancer therapy in young female cancer patients. We and others have previously demonstrated that doxorubicin (DOX), one of the most widely used chemotherapeutic chemicals, has a dose-dependent toxicity on growing follicles. However, it is not fully understood if the primordial follicles are the direct or indirect target of DOX. Using both prepubertal and young adult female mouse models, we comprehensively investigated the effect of DOX on all developmental stages of follicles, determined the impact of DOX on primordial follicle survival, activation, and development, as well as compared the impact of age on DOX-induced ovarian toxicity. Twenty-one-day-old CD-1 female mice were intraperitoneally injected with PBS or clinically relevant dose of DOX at 10 mg/kg once. Results indicated that DOX primarily damaged granulosa cells in growing follicles and oocytes in primordial follicles and DOX-induced growing follicle apoptosis was associated with the primordial follicle overactivation. Using the 5-day-old female mice with a more uniform primordial follicle population, our data revealed that DOX also directly promoted primordial follicle death and the DNA damage-TAp63α-C-CASP3 pathway was involved in DOX-induced primordial follicle oocyte apoptosis. Compared to 21-day- and 8-week-old female mice that were treated with the same dose of DOX, the 5-day-old mice had the most severe primordial follicle loss as well as the least degree of primordial follicle overactivation. Taken together, these results demonstrate that DOX obliterates mouse ovarian reserve through both primordial follicle atresia and overactivation and the DOX-induced ovarian toxicity is age dependent.

1. Introduction

The remarkable advances of early cancer diagnosis and therapeutic regimens allow many patients to live long and productive lives after cancer. Recently, there are more concerns regarding the side effects during and following anti-cancer treatments (Woodward et al., 2011). Among prepubertal, adolescent, and young adult female cancer patients, ovarian toxicity and infertility are major side effects of cancer therapy. The ovary is composed of follicles at various developmental stages, which act as the basic functional unit. There is a finite number of primordial follicles set just after birth and these follicles remain in a quiescent state to represent the ovarian reserve, a marker of fertility potential. With advancing age, primordial follicles are activated in regular waves and develop to growing follicles, including primary, secondary, and antral stages, to support hormone secretion, oocyte

maturation, and ovulation from birth until menopause, when the primordial follicle pool is depleted. Both chemotherapy and irradiation have been reported to have highly detrimental impacts on the ovary and increase the risk of premature ovarian failure (POF), early menopause, and sub- or in-fertility (Meirow and Nugent, 2001; Molina et al., 2005; De Bruin et al., 2008; Morgan et al., 2012; Levine et al., 2018).

Thus far, most of the studies investigating the adverse impact of chemotherapy on female ovarian function and fertility focus on alkylating agents (Gonfloni et al., 2009; Kalich-Philosoph et al., 2013; Kim et al., 2013; Goldman et al., 2017; Kim et al., 2019; Nguyen et al., 2018). Equally as important as these alkylators, however, are the other types of anti-cancer drugs that are also widely used but may exhibit different ovarian toxic mechanisms. Chemotherapeutic chemicals can be grouped based on their cytotoxicities, including alkylating agents, antimetabolites, and topoisomerase poisons, etc. Although the majority

^{*} Corresponding author at: 915 Greene St, Rm 327, Columbia, SC 29208, USA E-mail address: sxiao@mailbox.sc.edu (S. Xiao).

of these chemicals kill cancer cells by inducing DNA damage and subsequent apoptosis, the precise mechanisms are not the same (Cheung-Ong et al., 2013). It is therefore expected that different chemotherapeutic chemicals may exhibit different cytotoxic activities to non-tumorous tissues, including the ovary. For example, cyclophosphamide, one of the most widely used alkylating agents, primarily damages mitotically active granulosa cells of growing follicles, which subsequently overactivates dormant primordial follicles and exhausts ovarian reserve (Kalich-Philosoph et al., 2013; Goldman et al., 2017). In contrast, cisplatin, a platinum containing anti-cancer agent, directly promotes the apoptosis of oocytes in primordial follicles, leading to POF (Gonfloni et al., 2009; Kim et al., 2013; Kim et al., 2019; Nguyen et al., 2018; Tuppi et al., 2018). Therefore, blocking key factors of the pathways of primordial follicle activation and apoptosis protects ovarian reserve and fertility from the exposure of cyclophosphamide and cisplatin, respectively (Gonfloni et al., 2009; Kalich-Philosoph et al., 2013; Kim et al., 2013; Goldman et al., 2017; Kano et al., 2017; Kim et al., 2019; Nguyen et al., 2018; Tuppi et al., 2018). These data strongly support that there are mechanistic differences in the induction of follicle damage and ovarian reserve depletion in response to different chemotherapies, thus requesting different fertility preservation strategies.

Doxorubicin (DOX), which is sold as the trade names of Adriamycin or Rubex, is a widely used anthracycline anti-tumor antibiotic (Blum and Carter, 1974). DOX damages cancer cells as a poison to topoisomerase II (TOP2), a critical enzyme to regulate DNA topology (Nitiss, 2009). It can bind to TOP2 and form DOX-TOP2-DNA covalent complexes which blocks subsequent DNA religation, generating a high level of DDSBs that activate downstream DNA damage responses and cell apoptosis (Minotti et al., 2004). DOX is frequently used in combination with bleomycin, vinblastine, and with or without dacarbazine (ABVD or ABV, A indicates Adriamycin or DOX) for treating Hodgkin's lymphoma and many other cancers (Molnar et al., 1997). The reproductive toxicity of ABVD or ABV treatment was reported somewhat controversial (De Bruin et al., 2008; Decanter et al., 2010; Harel et al., 2011; Sonigo et al., 2016; McLaughlin et al., 2017; Poirot et al., 2017; Sonigo et al., 2017). More importantly, the impact of each individual chemotherapeutic drug on female ovarian function and fertility has been rarely studied, but these compounds are frequently used as a single agent to treat malignancies in women of reproductive age and prepubertal girls. With respect to DOX, the administration of a single agent of DOX is used as the first-line chemotherapeutic regimen for multiple malignant tumors such as lymphoma, leukemia, soft tissue sarcoma, and breast cancer, etc (National Cancer Instititue, 2007; Cortazar et al., 2012; Food and Administration, 2016; Seddon et al., 2017).

Using both the 3D in vitro follicle culture model and in vivo mouse model, we and others have demonstrated that DOX has a dose-dependent toxicity on growing follicle development, steroid hormone synthesis and secretion, and oocyte maturation and ovulation (Perez et al., 1997, Ben-Aharon et al., 2010, Ben-Aharon, Bar-Joseph et al., 2010, Roti Roti and Salih, 2012, Xiao et al., 2017, Wang et al., 2018). However, it is not fully understood if the primordial follicles are the direct or indirect target of DOX. Using both prepubertal and young adult female mouse models, we aimed to comprehensively investigate the effect of DOX on all developmental stages of follicles within an intact ovary, to determine the impact of DOX on primordial follicle survival, activation, and development, as well as to compare the impact of age on DOX-induced ovarian toxicity.

2. Materials and methods

2.1. Animals and treatments

All procedures involving mice were approved by the Institutional Animal Care and Use Committee (IACUC) at the University of South Carolina (USC). The CD-1 mouse breeding colony was purchased from Charles River Laboratory (Wilmington, MA) and maintained in the

animal facility of USC, with free access to food and water, under a 12 h light/dark cycle (6:00 AM to 6:00 PM) at 22 °C \pm 1 °C with 40-60% humidity. All the mice we used in this study were bred and maintained in the same environment. The pregnant females were checked every morning and every evening to record the accurate date of birth of the pups. All the pups were weaned on postnatal day (PND) 20 and the female offspring from the same litter were housed with 3-5 mice per cage and were randomly distributed into different experimental groups. In humans, the DOX treatment dosage ranges from 8 to 400 mg/m², equivalent to 0-10 mg/kg, which depends on the body size, cancer type, and disease condition (Scheithauer et al., 1985; Ferguson et al., 1993). Twenty-one-day-old female mice include all classes of follicles and have not started the estrous cyclicity, which allows us to evaluate the impact of DOX exposure on all developmental stages of follicles without the disruption of hormonal change. Meanwhile, since a significant number of prepubertal and adolescent young female cancer patients are exposed to chemotherapeutics including DOX, the 21-dayold female mice can represent this specific population. Therefore, the 21-day-old female mice were treated with a single intraperitoneal (i.p.) injection of a human relevant dose of DOX at 10 mg/kg body weight. The DOX was dissolved in 1 x phosphate buffered saline (1xPBS or PBS, pH = 7.4), thus, the i.p. injection of the same volume of PBS was used as the control. The ovaries were harvested on 1, 4, 7, and 14 days after PBS or DOX injection for a comprehensive evaluation of DOX on ovarian follicle survival, activation, and development. Our follicle counting results showed that > 95% of primordial follicle loss occurred within 4 days after DOX treatment. Therefore, we decided to investigate whether the same dose of DOX could induce the same degree of primordial follicle loss in 5-day-old and 8-week-old mice within 4 days post treatment. The 5-day-old female mice with a more uniform primordial follicle population received the same PBS or DOX exposure strategy to study the effect of DOX on primordial follicle survival, activation, and development. For 5-day-old mice, the ovaries were collected on days 1 and 3 post PBS or DOX treatment because the DOXtreated mice were very weak on day 4, ensuring animal welfare. The 8week-old female mice were also treated with the same dose of PBS or DOX, and the ovaries were harvested on days 1 and 4 to determine the effect of age on DOX-induced ovarian reserve obliteration. Additionally, to avoid the potential influence of hormonal changes at different stages of the estrous cycle, the estrous cycle stage of 8-week-old female mice was monitored using vaginal cytology as we previously described (Zhao et al., 2013), and all the mice were injected with PBS or DOX at the diestrus stage. There were 4-6 mice in each treatment, time point, and age group.

2.2. Histology and follicle counting

The collected ovaries were fixed in Shandon™ Formal-Fixx™ 10% Neutral Buffered Formalin solution (ThermoFisher Scientific, Waltham, MA) for 24 h (h), embedded in paraffin, and sectioned at the thickness of 5 µm with a RM 2165 microtome (Leica Microsystems, Nussloch, Germany). Ovarian sections were stained with hematoxylin and eosin (H&E, ThermoFisher Scientific, Waltham, MA) at every 5th section for histological evaluation and follicle counting. Blinded follicle counting was performed for each ovary by counting the follicles containing oocytes with a visible nucleus. Different developmental stages of follicles were classified according to accepted published standards (Pedersen and Peters, 1968; Goldman et al., 2017). Briefly, the primordial follicle was defined as an oocyte surrounded by one layer of squamous granulosa cells; the primary follicle possessed an oocyte surrounded by a single layer of cuboidal granulosa cells; the secondary follicle was defined as an oocyte surrounded by two or more layers of cuboidal granulosa cells with no visible antrum; and the antral follicle was defined as an oocyte surrounded by five or more layers of granulosa cells with no visible antrum or contain a clearly defined antral space. Atretic secondary and antral follicles were defined by the appearance of > 10%

of pyknotic granulosa cells and/or degenerated oocytes following the previous published method (Brown et al., 2010; Winship et al., 2018). Early-growing primordial follicles were characterized by an enlarged oocyte with a diameter $> 22 \, \mu m$, the average of oocyte size in primary follicles, but was surrounded by one layer of flattened granulosa cells (Castrillon et al., 2003). Additionally, adjacent ovarian sections were also evaluated to ensure each follicle was only counted once.

2.3. Oocyte diameter measurement

The accurate calculation of oocyte diameter was ensured by using the DP2-BSW software (Olympus, Tokyo, Japan) after calibration with a stage micrometer (Gurley Precision Instruments, Troy, NY). The oocyte with a clear visible nucleus was selected for the following measurement and 20 oocytes from each developmental stage of follicles were included. Four mice from the control group of 21-day-old mice were used for the measurement of oocyte diameters of primordial, primary, secondary, and antral stages of follicles. Another 4 mice from the DOX treatment group of 21-day-old mice were used for the measurement of oocyte diameters of early-growing primordial follicles. The oocyte diameter was measured from the inner layer of granulosa cells including the zona pellucida, when present. Additionally, two measurements were performed for each oocyte: the first measurement detected the widest diameter of the oocyte and the second measurement originated at a right angle from the midpoint of the first measurement. Then, these two measurements were averaged and used as the final oocyte diameter.

2.4. TUNEL assay

The DeadEnd Thurston Fluorometric TUNEL System Kit (Promega, Madison, MI) was used to detect apoptotic cells according to the manufacturer's instructions. Briefly, paraffin sections were deparaffinized, rehydrated, and fixed in 4% formaldehyde in PBS. After permeabilizing by 20 $\mu g/ml$ Proteinase K solution for 10 min, the TdT reaction mix was added to the ovarian sections and incubated for 1 h at 37 °C in a humidified chamber. The sections were counter-stained using Vectashield Mounting Medium with DAPI (Vector Laboratories, Burlingame, CA) and TUNEL positive cells were analyzed under the fluorescence microscope.

2.5. Immunohistochemistry and immunofluorescence

The expression of MSY2, p-AKT, Foxo3a, phopho-p63, and cleaved caspase 3 (C-CASP3) in the ovaries treated with PBS or DOX at different time points was determined by immunohistochemistry (IHC). Briefly, ovarian sections were deparaffinized in xylene and rehydrated in a series of graded ethanol baths (100%, 95%, 80%, 70%, and 50%). Antigen retrieval was performed by microwaving ovarian sections for 15 min in 0.01 M sodium citrate medium (pH = 6). Slides were incubated in 3% hydrogen peroxide (ThermoFisher Scientific, Waltham, MA) followed by incubating in blocking solution (2% BSA diluted in PBS) for 1 h at room temperature (RT) and then incubated for 2 h at 4 °C with the primary antibody. Then, slides were rinsed using PBS and incubated in 1:500 dilution of the secondary antibody (Goat anti-rabbit IgG (HRP), ab6271 or Goat anti-mouse IgG H&L (HRP), ab6789, Abcam, Cambridge, MA) for 1 h at RT. The sections were washed and then incubated with DAB substrate kit (ab64238, Abcam, Cambridge, MA), and counterstained with hematoxylin. The immunofluorescense (IF) was used to detect the expression level of gamma-H2A.X (γ-H2AX) in the 5-day-old ovaries treated with PBS or DOX at 3, 6, 12, and 24 h. The protocol was similar to the IHC except omitting the hydrogen peroxide incubation until primary antibody incubation. Ovarian sections were incubated with Donkey anti-Mouse IgG (H + L) Highly Cross-Adsorbed Secondary Antibody, Alexa Fluor 546 (A10036, 1:500, ThermoFisher Scientific, Waltham, MA) in blocking solution for 1 h at RT. The slides were then mounted with Vectashield containing DAPI

(Vector Laboratories, Burlingame, CA). Negative control sections were treated the same but the primary antibody was replaced with goat antirabbit IgG or goat anti-mouse IgG (1:200, Abcam, Cambridge, MA). Primary antibodies against γ-H2AX (phospho Ser 139) (ab26350, 1:200) and AKT1 (phosphor S473) (ab81283, 1:200) were purchased from Abcam (Cambridge, MA); cleaved-caspase 3 (GTX22302, 1:200) was purchased from GeneTex (Irvine, CA); Foxo3a (10849–1-AP, 1:200) was purchased from Proteintech (Chicago, IL); phopho-p63 (Ser160/162) (4981S, 1:200) was purchased from Cell Signaling Technology (Danvers, MA), and MSY2 (1:1000) was a gift from Dr. Teresa Woodruff at Northwestern University.

2.6. Western blot

The postnatal day (PND) 5 mouse ovaries were harvested at 3, 6, 12, and 24 h after PBS or DOX treatment and placed in dry ice immediately at the time of harvest. The ovaries were homogenized in ice-cold Laemmli sample buffer (Bio-Rad, Hercules, CA) containing protease and phosphatase inhibitor cocktail (ThermoFisher Scientific, Waltham, MA) and separated by Sodium Dodecyl Sulfate Polyacrylamide Gel Electrophoresis (SDS-PAGE, 12% acrylamide gel). Proteins were transferred to the $0.45\,\mu m$ nitrocellulose blotting membrane (GE Healthcare Life Science, Pittsburgh, PA). After blocking with 5% BSA dissolved in Tris-buffered saline containing 0.1% Tween-20 (TBST), the membranes were incubated with primary antibodies overnight at 4°C. After washing with TBST, membranes were incubated with appropriate secondary antibodies conjugated to horseradish peroxidase at a dilution of 1:2000 for 1 h at RT. The protein was then detected using Pierce™ ECL Western Blotting Substrate Kit (ThermoFisher Scientific, Waltham, MA) according to the manufacturer's instructions. The primary antibodies we used were anti-γ-H2AX (phosphor Ser 139) (1:1000, ab26350, Abcam, Cambridge, MA); anti-TAp63α (1:1000, gift from Dr. So-Youn Kim at Nebraska University Medical Center), and anti-β-actin (1:1000, ab6276, Abcam, Cambridge, MA).

2.7. DOX fluorescence detection

DOX accumulation and distribution in the ovary were determined based on its autofluorescence as we previously described (Xiao et al., 2017). An examination time window of 72 h was selected to cover all the changes of DOX accumulation in the ovaries. Briefly, ovarian sections were deparaffinized in xylene and rehydrated in a series of graded ethanol baths (100%, 95%, 80%, 70%, and 50%). The slides were then mounted with Vectashield containing DAPI (Vector Laboratories, Burlingame, CA). Next, images from 5-day-old mice treated with PBS or DOX for 3, 6, 12, 24, and 72 h were taken using a 40 X objective using a fluorescence microscope with a Lumen 200 Fluorescence Illumination System (Prior Scientific Inc., Rockland, MA).

2.8. Statistical analysis

Data are presented as means \pm S.D. The follicle counting data were analyzed using one-way analysis of variance (ANOVA) followed by Tukey's post hoc test for a comparison of means between more than two independent groups and an unpaired t-test with Welch's correction for detecting the difference between two groups. All the statistical comparisons were performed using PRISM 7.0 (GraphPad Software, Inc., La Jolla, CA). The significance level was set at P < .05.

3. Results

3.1. DOX exhibited distinct cytotoxicities in different follicular cell types and developmental stages of follicles

We first characterized the comprehensive impact of DOX on an intact ovary including all classes of follicles by injecting 21-day-old CD-1

0 ⊥ day

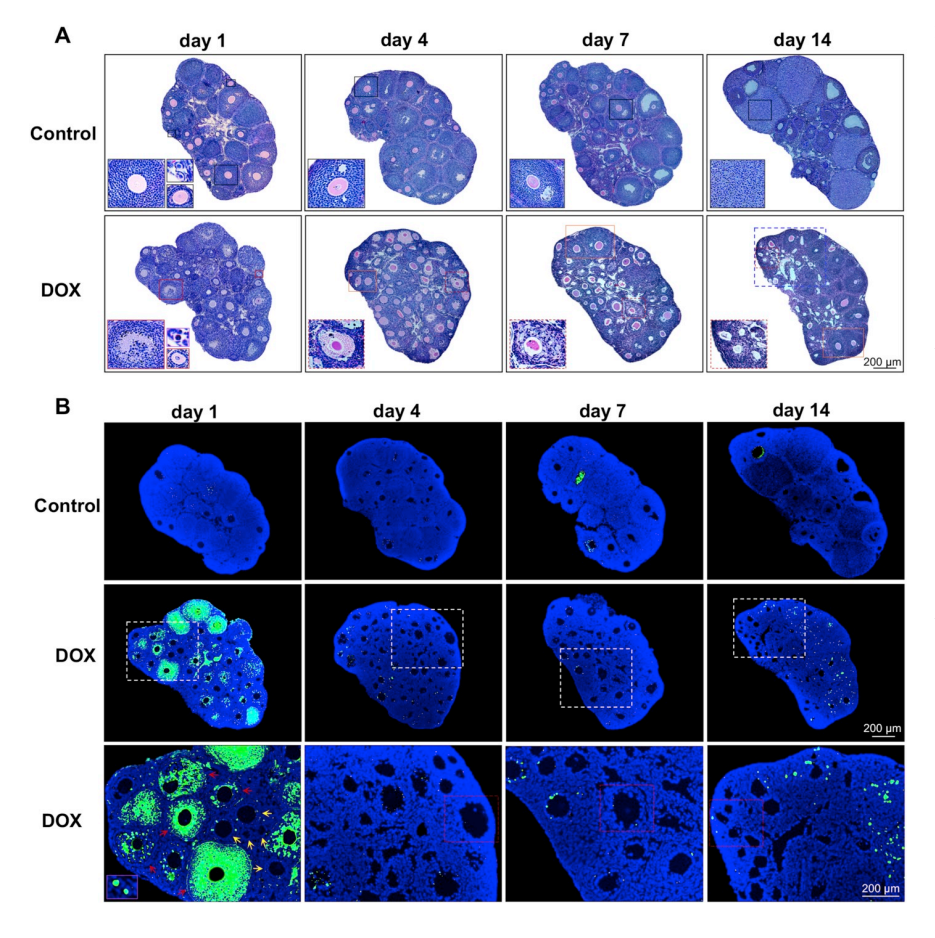
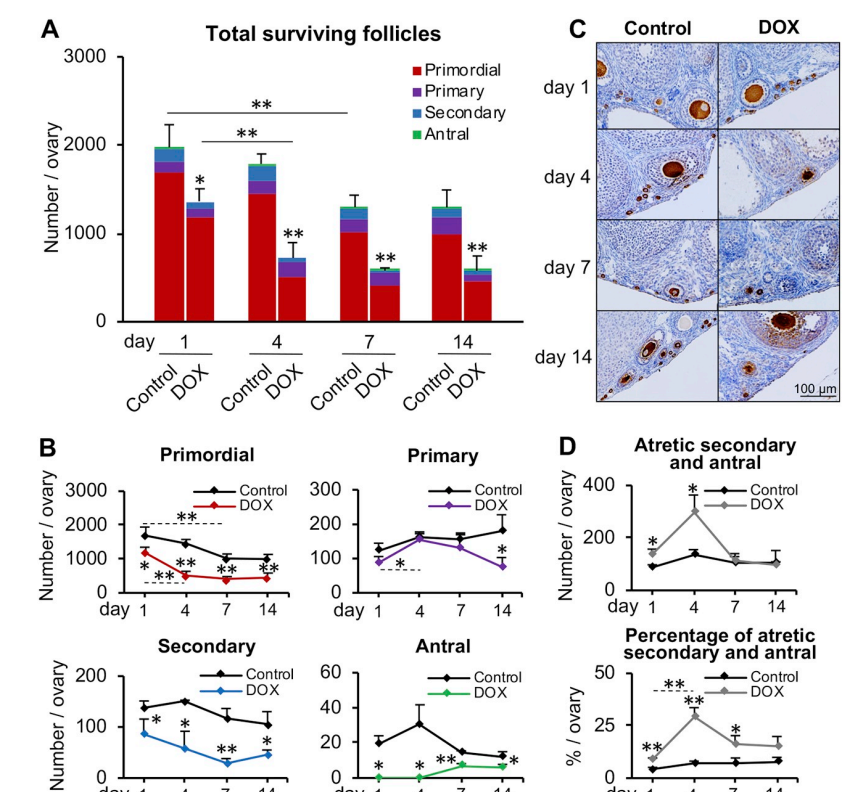


Fig. 1. The ovarian toxicity of DOX was cell type and follicle developmental stage dependent. (A) Representative ovary histological images on days 1, 4, 7, and 14 after PBS or DOX treatment. Black squares indicate normal follicle morphology on day 1, 4, and 7 and existence of corpus luteum (CL) on day 14 in PBS-treated ovaries; red squares indicate apoptotic granulosa cells in growing follicles after DOX treatment; purple square indicates apoptotic oocyte in primordial follicles after DOX treatment on day 1; red dash squares indicate degenerated growing follicles on days 4, 7, and 14 after DOX treatment; and orange squares indicate newly developed follicles in DOX-treated ovaries on days 7 and 14. (B) Representative ovary TUNEL staining images on days 1, 4, 7, and 14 after PBS or DOX treatment. Purple squares indicate apoptotic oocytes in primordial follicles in DOX-treated ovaries on day 1; red dash squares indicate degenerated growing follicles that were corresponding to the degenerated follicles in (A); white dash squares were corresponding to images below with higher magnification. N = 5-10 female mice in each treatment group and 3-5 replicates of histology and TUNEL staining were performed. (For interpretation of the references to colour in this figure legend, the reader is referred to the web version of this article.)



day

Fig. 2. DOX diminished ovarian reserve in 21-day old female mice. (A) Total number of all classes of surviving follicles per ovary on days 1, 4, 7, and 14 after PBS or DOX treatment. (B) Total number of specific developmental stage of follicles per ovary on days 1, 4, 7, and 14 after PBS or DOX treatment. (C) Expression of MSY2 (brown staining, an oocyte cytoplasmspecific protein) examined by immunohistochemistry (IHC) in PBS- and DOX-treated ovaries on days 1, 4, 7, and 14. (D) Total number and percentage of atretic secondary and antral follicles per ovary. *p < .05 and **p < .01 compared to the control group or the follicle number on another day after PBS or DOX treatment. Error bar: standard deviation. N = 5-10female mice in each treatment group and 3 replicates of IHC were performed. (For interpretation of the references to colour in this figure legend, the reader is referred to the web version of this article.)

female mice with PBS or a clinically relevant dose of DOX at 10 mg/kg once. Ovaries were harvested on days 1, 4, 7, and 14 for histology and TUNEL assay. On day 1 after treatment, both histology and TUNEL results revealed that the DOX-treated ovaries had a markedly increased granulosa cell apoptosis in the primary, secondary, and antral stages of follicles, demonstrated by the condensed granulosa cell cytoplasm and pyknotic and fragmented nuclei based on histological staining, as well as the DNA fragmentation based on positive TUNEL staining (Fig. 1A, red squares; Fig. 1B, red and yellow arrows). However, no evident damages were noted in the oocytes of these apoptotic growing follicles (Fig. 1A). Compared to primary and two-layered secondary follicles (Fig. 1B, yellow arrows), the degree of granulosa cell apoptosis was more severe in multilayered secondary and antral stages of follicles (Fig. 1B, red arrows). Different from the pattern of DOX-induced apoptosis of growing follicles, DOX primarily induced oocyte apoptosis in primordial follicles, but with pre-granulosa cells showing similar morphology to the control group (Fig. 1, purple squares). From day 4 to 14, a majority of apoptotic follicles at secondary and antral stages in DOX-treated ovaries had complete degenerated granulosa cell layers, with some showing distorted or degenerated oocytes (Fig. 1, red dash squares). Moreover, these DOX-treated ovaries had some newly developed secondary and early antral follicles (Fig. 1A, orange squares). These results demonstrate that DOX exhibits distinct cytotoxicities between somatic and germ cells as well as among different developmental stages of follicles.

3.2. DOX induced primordial follicle loss and diminished ovarian reserve

Follicle counting was next performed to quantify the effect of DOX on the survival, activation, and development of all classes of follicles. There was a natural loss of 9.47% (1974.67 \pm 256.80 vs 1787.67 \pm 112.43), 34.30% (1974.67 \pm 256.80 vs 1297.33 \pm 136.15), and 34.39% (1974.67 \pm 256.80 vs 1295.67 \pm 197.18) of total surviving follicles in the control group from day 1 to days 4, 7, and 14, respectively (Fig. 2A). The significant follicle losses on days 7 and 14, corresponding to the mouse age of days 28 and 35, suggests a physiological follicle loss during peripubertal period. Compared to PBS-treated ovaries, the numbers of total surviving follicles in the DOX-treated ovaries were reduced by 30.93% (1974.67 \pm 256.80 vs 1364.00 \pm 141.92), 59.63% (1787.67 \pm 112.43 vs 721.67 \pm 174.50), 55.34% (1297.33 \pm 136.15 vs 579.33 \pm 30.53), and 55.47% (1295.67 \pm 197.18 vs 577.00 \pm 168.32) on days 1, 4, 7, and 14 post-DOX injection, respectively (Fig. 2A), implying that there was significant extra follicle death upon DOX treatment.

After classifying these follicles based on specific developmental stages, the numbers of primordial follicles in DOX-treated ovaries were significantly lower than PBS-treated ovaries at all examining time points (Fig. 2B), with > 95% of primordial follicle loss occurred within 4 days after DOX treatment. The immunostaining results of MSY2, an oocyte cytoplasm-specific protein, confirmed the primordial follicle loss after DOX treatment (Fig. 2C). The number of primary follicles in DOXtreated ovaries was reduced by 27.46% (122 \pm 22.52 vs 88.5 ± 17.14) on day 1 compared to the control group, however, it was greatly increased by 74.39% (88.5 \pm 17.14 vs 154.33 \pm 17.79) from day 1 to day 4 with the absolute primary follicle number being similar to PBS-treated ovaries (Fig. 2B). The raised number of primary follicles from day 1 to day 4 after DOX treatment suggests that the loss of growing follicles may trigger an overactivation of dormant primordial follicles as described in previous studies using other chemotherapeutic chemicals (Kalich-Philosoph et al., 2013; Chang et al., 2015; Goldman et al., 2017), which will be discussed in the next section. Consistent with the results of histology and TUNEL assay (Fig. 1) and the significantly increased atretic secondary and antral follicles (Fig. 2D), the numbers of surviving secondary and antral follicles were significantly lower than PBS-treated ovaries at all examining time points (Fig. 2B). More specifically, the number of secondary follicles in DOX-treated ovaries showed a continuous decrease from day 1 to day 7

but was then significantly increased by 60.92% (29.00 \pm 9.17 vs 46.67 ± 8.33) from day 7 to day 14 (Fig. 2B). There was no surviving antral follicle on days 1 and 4 but some preantral follicles developed to antral stage on days 7 and 14 (Fig. 2B). The increased number of secondary follicles from day 7 to day 14 and the reappearance of antral follicles on days 7 and 14 indicate that the newly recruited and/or survived preantral follicles develop to secondary and antral stages. Moreover, because the numbers of primary, secondary, and antral follicles in DOX-treated ovaries were still less than control group, it was proposed that the newly recruited and grown follicles cannot compensate for the loss of same stage of follicles upon DOX treatment.

3.3. DOX promoted primordial follicle overactivation

Since the follicle counting results showed significantly elevated numbers of primary follicles on days 4 and 7 after DOX treatment (Fig. 2B), we next examined whether the DOX will overactivate dormant primordial follicles. Compared to PBS-treated ovaries, histological results showed that the DOX-treated ovaries on day 1 contained significantly more of transient stage of primordial follicles, which were characterized by an enlarged oocyte surrounded by one layer of flattened pre-granulosa cells (Fig. 3A, black square and 3B). The morphological appearance of these follicles is similar to the follicles with oocytes lacking Pten, Foxo3a, and Tsc1, three essential repressors of primordial follicle activation (Castrillon et al., 2003, Reddy et al., 2005, Adhikari et al., 2009, Adhikari and Liu, 2010, Adhikari, Zheng et al. 2010), and they were thus termed early-growing primordial follicles. After separating early-growing primordial follicles from normal primordial follicles, the numbers of early-growing primordial follicles in DOX-treated ovaries were significantly higher than PBS-treated ovaries on days 1, 4, and 7 and then dropped to a similar level on day 14 (Fig. 3C). These results reflect the fact that the elevated numbers of primary follicles on day 4 and secondary and antral follicles on days 7 and 14 in DOX-treated ovaries (Fig. 2B) was at least partially attributed to the newly recruited and activated primordial follicles. Interestingly, some early-growing primordial follicles in DOX-treated ovaries had their single layer of flattened pre-granulosa cells proliferated to 2-3 layers but did not transform to cuboidal granulosa cells on days 4 and 7 (Fig. 3A, red squares). Accordingly, most of these aberrantly developed follicles had degenerated oocytes on day 14 (Fig. 3A, orange squares), suggesting that these early-growing follicles underwent atresia if the flattened pre-granulosa cells did not normally differentiate into cuboidal granulosa cells.

3.4. DOX obliterated mouse ovarian reserve through both primordial follicle atresia and overactivation

Since the numbers of early-growing primordial follicles and increased primary follicles on day 4 were still substantially less than the number of primordial follicle loss (e.g. 95.08 vs 504.92 on day 1 after DOX treatment) and our histology and TUNEL results showed apoptotic oocytes in primordial follicles (Fig. 1), we next tested the hypothesis that DOX treatment can also directly damage primordial follicles. We chose 5-day-old CD-1 female mice for the same PBS and DOX treatment regimen because their ovaries have a more uniform primordial follicle population. Upon DOX treatment, the total surviving follicle numbers were significantly decreased by 82.96% (2372.67 \pm 217.20 vs 95.29% 404.33 ± 187.13) and (2200.67 ± 210.37) 103.67 ± 4.93) on day 1 and day 3 compared to the control group, respectively (Fig. 4A). After classifying follicles based on specific developmental stages, the numbers of primordial follicles in DOX-treated ovaries were significantly decreased by 83.81% and 96.29%, and the numbers of primary follicles were decreased by 55.52% and 47.41%, on day 1 and day 3 compared to the control group, respectively (Fig. 4B-4D). The majority of secondary follicles (93.43%) were lost on day 1 after DOX treatment and no secondary follicles were observed on day 3

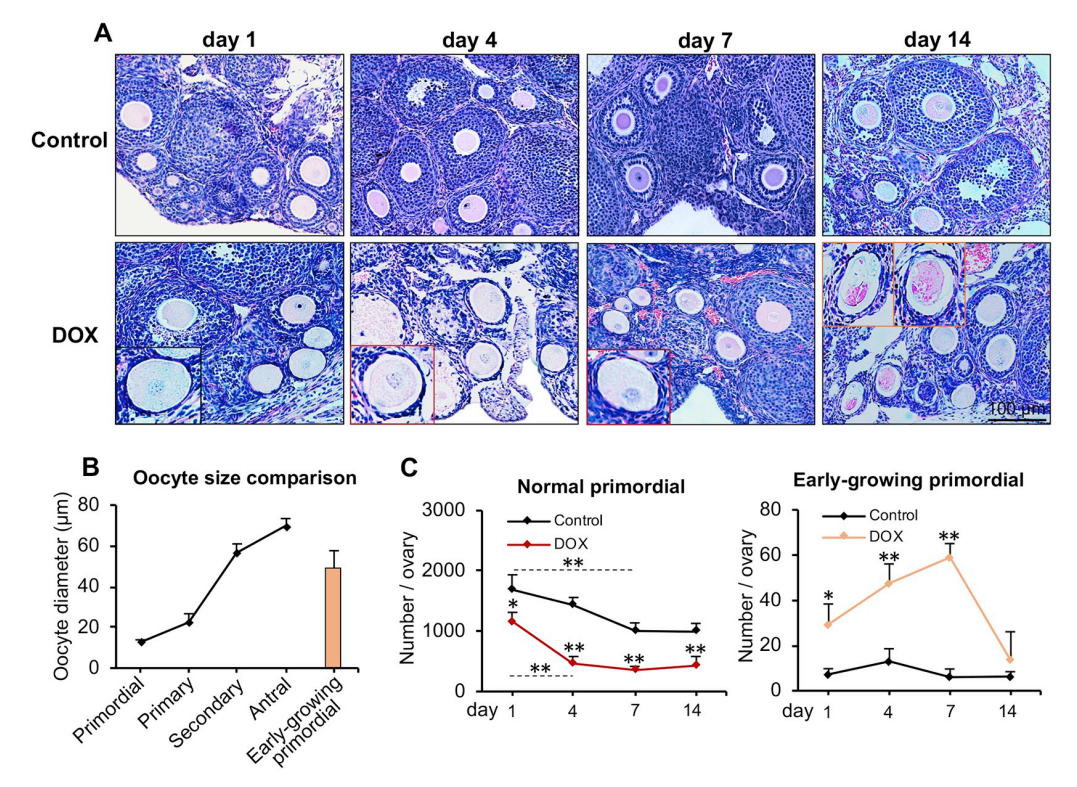


Fig. 3. DOX induced primordial follicle overactivation in 21-day old female mice. (A) Representative ovary histological images on days 1, 4, 7, and 14 after PBS or DOX treatment. The Black square indicates a representative early-growing primordial follicle with an enlarged oocyte surrounded by one layer of flattened pregranulosa cells on day 1; Red squares indicate early-growing primordial follicles with more than one flattened pre-granulosa cell layers on days 4 and 7; and orange squares indicate degenerated early-growing primordial follicles. (B) The average oocyte diameter in different developmental stages of follicles and in early-growing primordial follicles. (C) Total number of normal primordial and early-growing primordial follicles per ovary on days 1, 4, 7, and 14 in PBS- or DOX-treated ovaries. $^*p < .05$ and $^*p < .01$ compared to control group or the follicle number on another day after PBS or DOX treatment. Error bar: standard deviation. N = 5–10 female mice in each treatment group and 3 replicates for histological staining. (For interpretation of the references to colour in this figure legend, the reader is referred to the web version of this article.)

(Fig. 4B-4D). Moreover, the number of primary follicles in the control group was significantly decreased from day 1 to day 3. Considering the increased number of secondary follicles on day 3, these results indicated that primary follicles were developed into secondary follicles during this period. However, no significant decrease of primary follicles was found in the DOX-treated ovaries from day 1 to day 3, suggesting that some primordial follicles could be activated and recruited into the primary follicle pool which was similar to that in the 21-day-old mice. Consistent with the results from DOX-treated 21-day-old mice, the 5-day-old mice also showed significantly increased numbers of early growing primordial follicles after DOX treatment (Fig. 4B), particularly on day 3 (Fig. 4C, red arrows).

To confirm the primordial follicle overactivation, IHC was performed to detect the expression of p-AKT and Foxo3a, two essential regulators to maintain dormant oocytes in primordial follicles and critical markers to determine primordial follicle activation (Castrillon et al., 2003; Reddy et al., 2005; John et al., 2008). Results indicated that the expression level of p-AKT was significantly induced in the oocytes of primordial follicles 3 h post DOX treatment and then decreased at 12 h (Fig. 4E). Furthermore, a significant amount of primordial follicles showed decreased expression level of Foxo3a in oocyte nuclei 6 h after DOX treatment, a marker of primordial follicle activation (Fig. 4E). These results suggest that DOX induces primordial follicle activation through the AKT-Foxo3a pathway. Taken together, these results demonstrate that prepubertal DOX exposure obliterates mouse ovarian reserve through both primordial follicle atresia and overactivation.

3.5. DNA damage-TAp63α-C-CASP3 pathway was involved in DOX promoted primordial follicle atresia

To investigate the underlying molecular mechanism of DOX-induced primordial follicle death, we first examined the accumulation and distribution of DOX in the ovary based on its autofluorescence. Positive DOX fluorescence was visible in the ovarian somatic cells and germ cells 3 and 6 h post treatment, with notable increased signals at 12 h, and then the DOX's autofluorescence was significantly decreased at 72 h (Fig. 5A). These results reveal that DOX can penetrate somatic cell layers in the ovary and reach the oocytes of primordial follicles. Next, we detected the expression of γ-H2AX, a well-characterized biomarker of DDSB as well as the major mechanism of DOX's cytotoxicity on tumorous cells (Kurz et al., 2004; Kuo and Yang, 2008). Results indicated that DOX significantly increased the expression of γ-H2AX in ovarian epithelial cells and oocytes but not in pre-granulosa cells of primordial follicles (Fig. 5B), and the increased expression levels of γ -H2AX peaked at 6 h after DOX treatment (Fig. 5C, red arrow), indicating that DOX can induce DDSBs in oocytes of primordial follicles. Previous studies have reported that TAp63α functions to respond to DNA damage that results in its phosphorylation and subsequent oocyte apoptosis initiation in the primordial follicles (Kerr et al., 2012; Kim et al., 2013; Tuppi et al., 2018). The expression of phospho-p63 was significantly induced in oocytes of primordial follicles 3 h post DOX treatment (Fig. 5D). In addition, western blot results showed that TAp63α was hyper-phosphorylated in DOX-treated ovaries at 6 h after DOX treatment (Fig. 5C, yellow arrow). Accordingly, there were greatly increased positive signals of C-CASP3, a well-defined marker in the

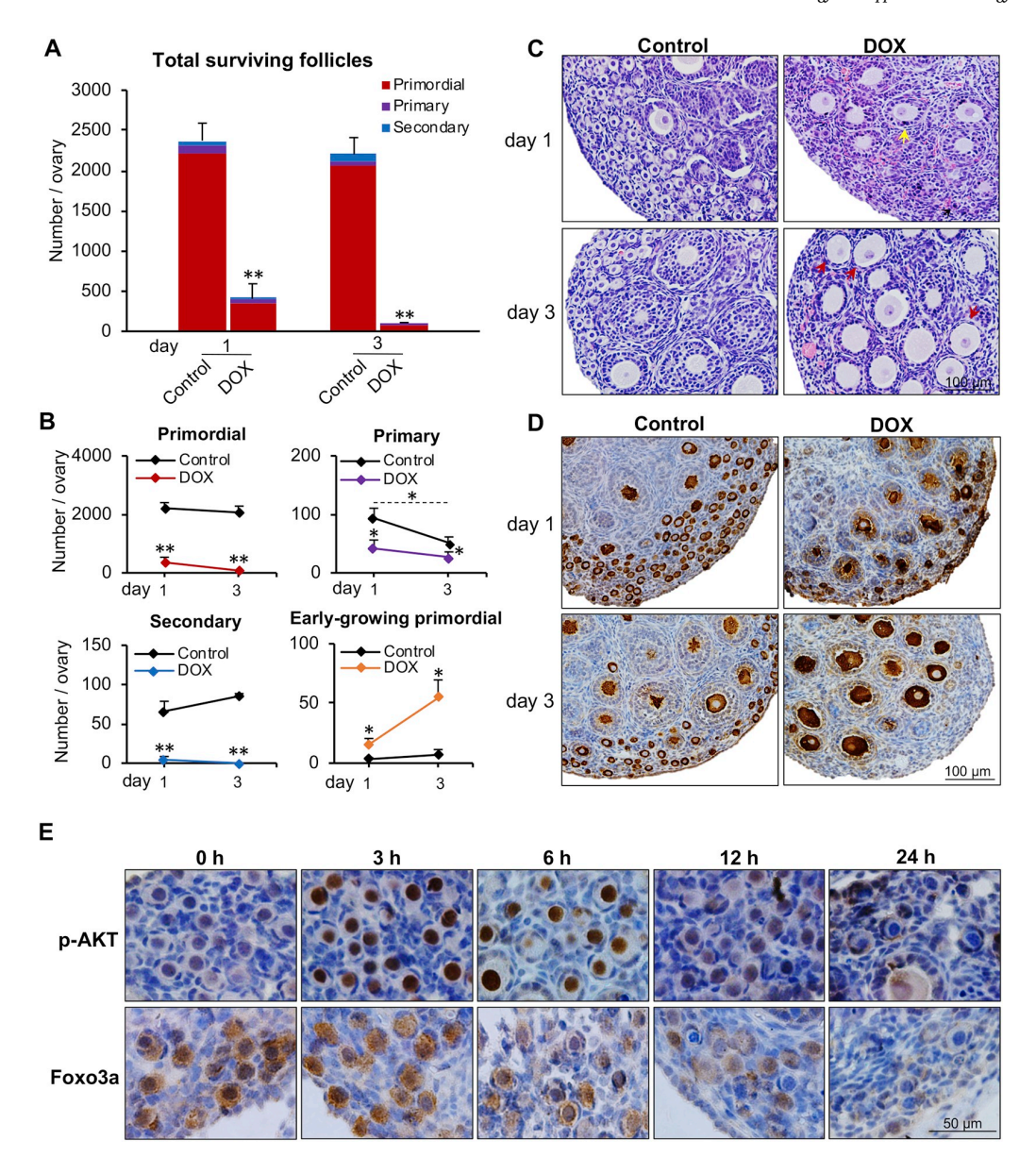


Fig. 4. DOX diminished ovarian reserve and induced primordial follicle overactivation in 5-day old mice. (A) Total number of all classes of surviving follicles per ovary on days 1 and 3 after PBS or DOX treatment. (B) Total number of specific developmental stage of follicles per ovary on days 1 and 3 after PBS or DOX treatment. (C) Representative ovary histological images on days 1 and 3 after PBS or DOX treatment. The Yellow arrow indicates a primary follicle with apoptotic granulosa cells on day 1 after DOX treatment and red arrows indicate early-growing primordial follicles on day 3 after DOX treatment. (D) Expression of MSY2 (brown staining, an oocyte cytoplasm-specific protein) examined by immunohistochemistry (IHC) in PBS- and DOX-treated ovaries on days 1 and 3. (E) Expression of p-AKT and Foxo3a (brown stainings) at 0, 3, 6, 12, and 24 h (h) after PBS or DOX treatment. *p < .05 and **p < .01 compared to control group or the follicle number on another day after PBS or DOX treatment. Error bar: standard deviation. N = 3-5 female mice in each treatment group and 3 replicates for histological staining and IHC were performed. (For interpretation of the references to colour in this figure legend, the reader is referred to the web version of this article.)

execution phase of cell apoptosis, from 12 to 24 h in oocytes of primordial follicles and granulosa cells after DOX treatment (Fig. 5E, red and yellow arrows). In summary, these results demonstrate that the DNA damage-TAp63 α -C-CASP3 pathway was involved in DOX-induced primordial follicle atresia.

3.6. DOX exhibited an age-dependent effect on primordial follicle atresia and overactivation

Since there was a different degree of DOX-induced primordial follicle loss between 5- and 21-day-old mice (83.81% in 5-day-old mice vs 29.79% in 21-day-old mice on day 1 after DOX treatment), 8-week-old adult CD-1 female mice were treated with the same dose of DOX to

study the effect of age on DOX-induced ovarian reserve obliteration. Compared to the control group, follicle counting results showed that the total surviving follicle numbers were significantly reduced by 41.83% (1330.67 ± 76.51) vs 774.00 ± 118.11 and 40.42% $(1320.33 \pm 90.12 \text{ vs } 786.67 \pm 51.07) \text{ on day 1 and day 4 after DOX}$ treatment in 8-week-old mice, respectively (Fig. 6A). After classifying these follicles based on specific developmental stages, the numbers of primordial, secondary, and antral follicles were all significantly reduced on days 1 and 4 after DOX treatment (Fig. 6B). However, the number of primary follicles was reduced by 23.88% on day 1, but it was then significantly increased to a similar amount to the control group on day 4 (Fig. 6B), indicating the overactivation of primordial follicles after DOX treatment. Interestingly, no early-growing primordial follicles

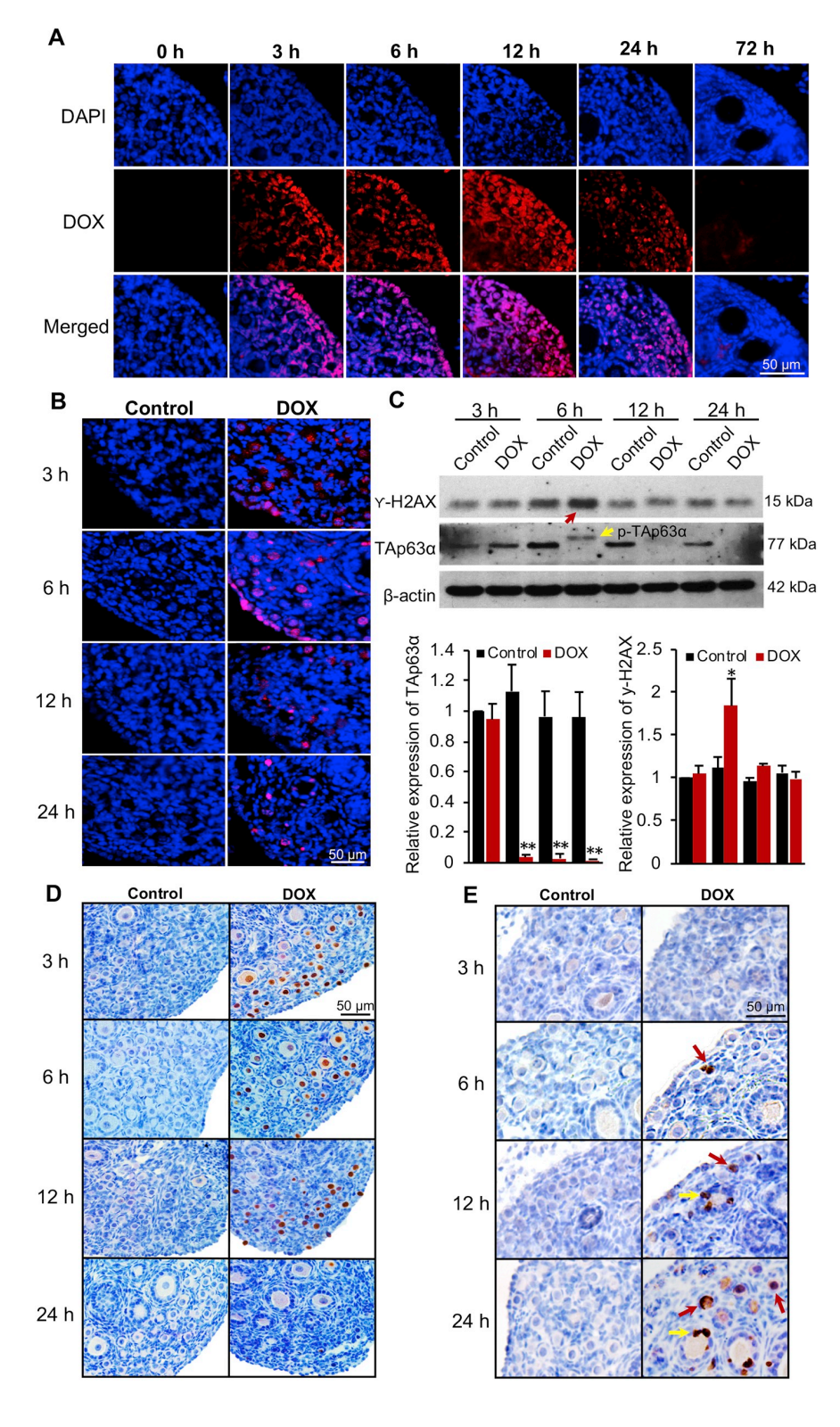


Fig. 5. DOX induced primordial follicle death through DNA damage-TAp63 α -C-CASP3 pathway. (A) Representative images of DOX autofluorescence (red) in the ovary at 0, 3, 6, 12, 24, and 72 h (h) after DOX treatment. (B) Ovarian expression of Gamma-H2AX (γ-H2AX, red staining) examined by immunofluorescence (IF) at 3, 6, 12, and 24 h after PBS or DOX treatment. (C) Expression of v-H2AX and hyper-phosphorylation of TAp63α examined by western blot in PBS- and DOX-treated ovaries at 3, 6, 12, and 24 h after PBS or DOX treatment. The histograms indicated the relative expression levels of TAp63 α and γ -H2AX comparing to β -actin. *p < .05and **p < .01 compared to the control group at the same time point after PBS or DOX treatment. Error bar: standard deviation. (D) Expression of phospho-(brown staining) examined by immunohistochemistry (IHC) at 3, 6, 12, and 24 h after PBS or DOX treatment. (E) Ovarian expression of Cleaved Caspase 3 (C-CASP3, brown staining) at 3, 6, 12, and 24 h after PBS or DOX treatment. N = 3-5 female mice in each treatment group and 3 replicates for IF, western blot, and IHC were performed. (For interpretation of the references to colour in this figure legend, the reader is referred to the web version of this article.)

were noted in 8-week old DOX-treated ovaries on day 1 and the amount of early-growing primordial follicles on day 4 was also significantly less than that in 5- and 21-day-old DOX-treated ovaries (Fig. 6C and D). Moreover, after comparing the percentages of primordial follicle loss between different ages of DOX-treated mice, it was found that the 5-day-old mice had the most severe primordial follicle loss compared to 21-day and 8-week-old mice (Fig. 6E). Taken together, these results

demonstrate that there is an age-dependent effect of DOX-induced primordial follicle atresia and overactivation.

4. Discussion

Using a 3D in vitro follicle culture model, we have previously demonstrated that DOX has a dose-dependent toxicity on growing follicle

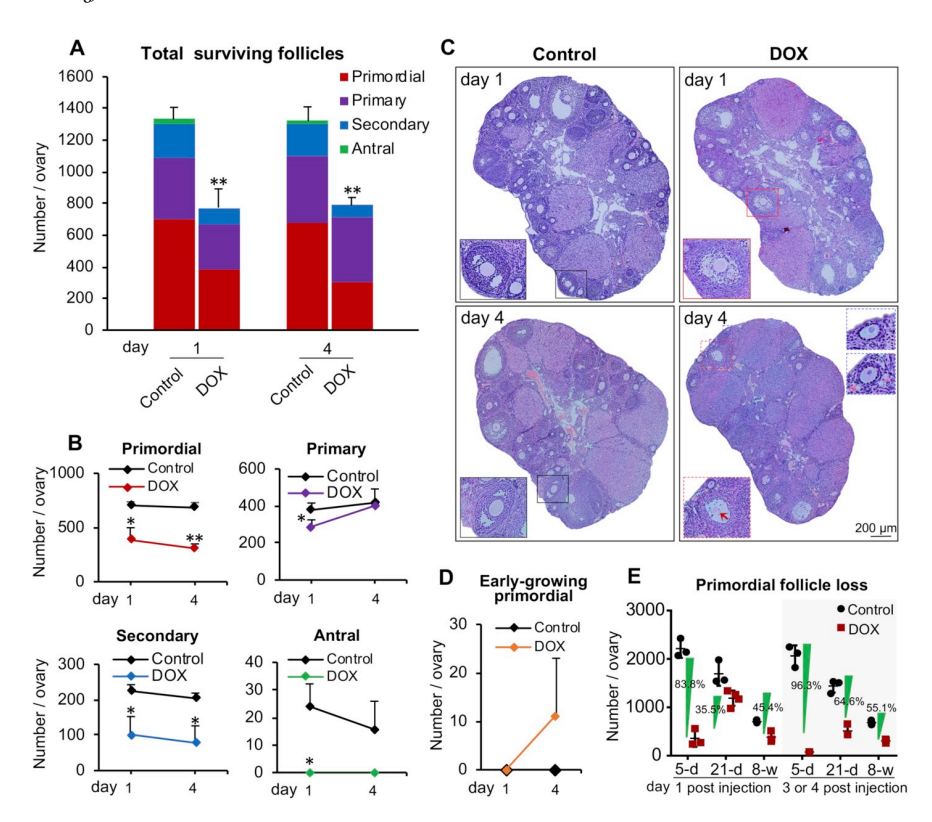


Fig. 6. DOX exhibited an age-dependent effect on primordial follicle atresia and overactivation. (A) Total number of all classes of surviving follicles per ovary on days 1 and 4 after PBS or DOX treatment in 8-week old female mice. (B) Total number of specific developmental stage of follicles per ovary on days 1 and 4 after PBS or DOX treatment. (C) Representative ovary histological images on days 1 and 4 after PBS or DOX treatment. Black squares indicate normal antral follicles in control groups; red square indicates an antral follicle with apoptotic granulosa cells on day 1 after DOX treatment; red dash square indicates an antral follicle with both apoptotic granulosa cells and degenerated oocyte on day 4 after DOX treatment; blue dash squares indicate early growing primordial follicles on day 4 after DOX treatment. (D) Total number of earlygrowing primordial follicles per ovary on days 1 and 4 in PBS- or DOX-treated ovaries. (E) Percentage of primordial follicle loss in different ages of DOXtreated mice. *p < .05 and **p < .01 compared to control group. Error bar: standard deviation. N = 4-6 female mice in each treatment group and 3 replicates for histological staining. (For interpretation of the references to colour in this figure legend, the reader is referred to the web version of this article.)

survival, hormone secretion, and oocyte maturation (Xiao et al., 2017). Here, we further used the whole animal model to comprehensively investigate the effect of DOX on all classes of follicles within an intact ovary. Consistent with our previous findings in vitro, DOX significantly increased apoptosis of growing follicles in all ages of DOX-treated animals. Moreover, we discovered that the granulosa cells, not oocytes, were the primary targets of DOX in the growing follicles. Further, the granulosa cells of more advanced stages of follicles such as multilayered secondary and antral follicles are more susceptible toward DOX-induced cytotoxicity than primary and two-layered secondary follicles are. These results are consistent with previous studies that the DOXinduced ovarian cell DNA damage and follicle apoptosis in the mouse ovary is in a cell- and follicle- type dependent manner (Roti Roti and Salih, 2012). It has been well characterized that upon primordial follicle activation, the one layer of granulosa cells of primary follicles will become mitotically active and proliferate multiple granulosa cell layers in the secondary and antral stages of follicles. Meanwhile, TOP2A is highly expressed in actively proliferating cancer cells, and forms DOX-TOP2-DNA covalent complexes, which generate high levels of DDSBs and activate subsequent cancer cell apoptosis (Minotti et al., 2004). In addition, dexrazoxane, a catalytic inhibitor of TOP2, protects mouse ovarian granulosa cells and marmoset monkey tissue from DOX's insult in vitro (Roti Roti and Salih, 2012; Salih et al., 2015). Therefore, these results demonstrate that the selective cytotoxicity of DOX on different types of follicular cells and different developmental stages of follicles is consistent with DOX's anti-cancer mechanism and is largely dependent on cell mitotic activity.

There are two major theories to explain the mechanism of primordial follicle depletion after anti-cancer treatments. First, chemotherapeutic chemicals, such as cyclophosphamide, primarily damage growing follicles, which further overactivates dormant primordial follicles, leading to an indirect effect of ovarian reserve burnout and POF (Kalich-Philosoph et al., 2013; Chang et al., 2015; Goldman et al., 2017). Second, some other anti-cancer agents, such as cisplatin, directly cause primordial follicle death and result in primordial follicle pool

obliteration (Gonfloni et al., 2009; Kim et al., 2013; Kim et al., 2019; Nguyen et al., 2018; Tuppi et al., 2018). In our study, the positive staining of DOX autofluorescence and the significantly increased DNA damage and apoptosis proteins suggest that DOX can directly induce primordial follicle death which is driven by the DNA damage-TAp63α-C-CASP3 pathway in the oocytes of primordial follicles. Moreover, our results also demonstrate that the DOX-induced growing follicle death promotes primordial follicle overactivation through the activation of AKT-Foxo3a pathway, a well-established signaling pathway to regulate oocyte dormancy in primordial follicles (Castrillon et al., 2003; Reddy et al., 2008). Based on these data, we conclude that DOX obliterates moue ovarian reserve through both primordial follicle atresia and overactivation. This discovery also explains the results from previous studies that the pharmacologic suppression of primordial follicle overactivation cannot entirely rescue the chemotherapy-induced primordial follicle pool depletion (Goldman et al., 2017; Kano et al., 2017). For the DOX-induced primordial follicle overactivation, Roti Roti et al. reported that ovarian stroma cells accumulated DOX and exhibited DNA damage before the granulosa cells, and they proposed that one possible mechanism contributing to the primordial follicle loss was the activation of primordial follicles induced by ovarian stroma remodeling (Roti Roti et al., 2012). Thus, the overactivation of primordial follicles observed in our study may be caused by the combination of growing follicle atresia, stroma demise, and direct stimulation. Previous studies indicated that DOX appeared in the ovary in a time-dependent manner with prevalence observed in the core stroma cells at early time points and then, DOX penetrated follicles (Roti Roti et al., 2012). In addition, the same study also showed that the DOX accumulation in the ovaries got a notable increase at 4 h and persisted through 48 h assay period. Our DOX distribution results demonstrated that the positive DOX fluorescence was visible in the ovarian stomal cells and oocytes 3 and 6 h post treatment, but with notable increased signals at 12 h and a significantly decrease at 72 h. The different DOX distribution patterns between previous data and our results might be caused by using the different age of mice (4-week-old vs 5-day-old) and dose of DOX (20 mg/kg vs 10 mg/kg). However, consistent with their conclusion (Roti Roti et al., 2012), the acute DOX accumulation pattern in the ovarian cortex region and the subsequent primordial follicle apoptosis indicate that the intervention approaches to protect ovarian reserve should be applied before or immediately after DOX treatment.

When cellular DNA damage occurs, the DNA damage checkpoint kinases of ATM (ataxia telangiectasia mutated) and/or ATR (ataxia telangiectasia and Rad-3 related) are activated through phosphorylation, which then activate a second wave of phosphorylation of CHEK1/ CHEK2 kinases and their downstream cell apoptotic pathway if the DNA damage is severe (Marechal and Zou, 2013). Regarding DNA damage in oocytes of primordial follicles, the priming checkpoint kinases of CHEK1/CHEK2 phosphorylate TAp63, which transforms the dimeric TAp63 to tetrameric conformation for activation of oocyte apoptosis (Tuppi et al., 2018; Kim et al., 2019). The specific pathway associated with TAp63 activation through ATR/CHEK1 and/or ATM/CHEK2 largely dependents on the type of anti-cancer therapies (Kim et al., 2019). Recent studies reported that TAp63 is phosphorylated via ATM/CHEK2 pathway when ovarian tissues are exposed to DOX in vitro (Tuppi et al., 2018). Consistent with their in vitro results, our in vivo data further confirm that DOX induces hyperphosphorylation of $TAp63\alpha$ in the oocytes of primordial follicles. Therefore, we propose that the adjuvant therapies to block the activation of ATM/CHEK2/TAp63α pathway should be considered to protect the DOX-induced oocyte apoptosis in primordial follicles.

Using three different ages of female mouse models, we, for the first time, discover that the degree of primordial follicle loss after exposure of DOX is age dependent. Both AMH and LH have been reported to protect mouse ovaries from chemotherapy-induced primordial death (Kano et al., 2017; Rossi et al., 2017). Since both AMH and LH have higher circulation levels in peripubertal and young adult mice than that at the juvenile stage(Bronson, 1981; Clark et al., 1997; Campbell et al., 2012), we propose that the lower levels of AMH and LH in 5-day-old mice make them more susceptible to the primordial follicle apoptosis after DOX treatment. Moreover, compared to adult female mice, the prepubertal mice have immature metabolic and detoxification capabilities in the liver, which is another possible reason for the age-dependent DOX-induced ovarian toxicities. These results suggest that the childhood cancer patients may be more susceptible toward cancer therapy-induced ovarian reserve obliteration and infertility than the adolescent and young adult female cancer patients. However, further studies are necessary to validate the age-dependent effect of DOX's ovarian toxicity in humans.

In summary, our studies demonstrate that the clinically relevant dose of DOX obliterates mouse ovarian reserve through both primordial follicle atresia and overactivation and DOX has an age-dependent ovarian toxicity pattern. These results indicate that DOX exposure during cancer therapy will significantly increase the risk of POF, early menopause, and sub- or in-fertility in young female cancer patients, and the adjuvant fertility protective regimen needs to target both primordial follicle atresia and primordial follicle overactivation.

Declaration of Competing Interest

The authors declare no conflict of interest.

Acknowledgements

This work was supported by the Arnold School of Public Health Start Up Fund at the University of South Carolina, National Science Foundation (NSF 1832910), National Institutes of Health (NIH P01ES028942 and K01ES030014) to S. Xiao, Science Undergraduate Research Fellowships (SURF) and Magellan Mini-Grant Award at the University of South Carolina to S. Johnson and S. Xiao, and National Institutes of Health (NIH P20GM103641) to S. Chatterjee, M. Nagarkatti, P. Nagarkatti, and S. Xiao. We greatly thank Dr. Teresa

Woodruff at Northwestern University and Dr. So-Youn Kim at the University of Nebraska Medical Center for the kind gift of MSY2 and $TAp63\alpha$ antibodies and helpful suggestions on the experimental design.

References

- Adhikari, D., Liu, K., 2010. mTOR signaling in the control of activation of primordial follicles. Cell Cycle 9 (9), 1673–1674.
- Adhikari, D., Flohr, G., Gorre, N., Shen, Y., Yang, H., Lundin, E., Lan, Z., Gambello, M.J., Liu, K., 2009. Disruption of Tsc2 in oocytes leads to overactivation of the entire pool of primordial follicles. Mol. Hum. Reprod. 15 (12), 765–770.
- Adhikari, D., Zheng, W., Shen, Y., Gorre, N., Hamalainen, T., Cooney, A.J., Huhtaniemi, I., Lan, Z.J., Liu, K., 2010. Tsc/mTORC1 signaling in oocytes governs the quiescence and activation of primordial follicles. Hum. Mol. Genet. 19 (3), 397–410.
- Bar-Joseph, H., Ben-Aharon, I., Rizel, S., Stemmer, S.M., Tzabari, M., Shalgi, R., 2010. Doxorubicin-induced apoptosis in germinal vesicle (GV) oocytes. Reprod. Toxicol. 30 (4), 566–572.
- Ben-Aharon, I., Bar-Joseph, H., Tzarfaty, G., Kuchinsky, L., Rizel, S., Stemmer, S.M., Shalgi, R., 2010. Doxorubicin-induced ovarian toxicity. Reprod. Biol. Endocrinol. 8, 20.
- Blum, R.H., Carter, S.K., 1974. Adriamycin. A new anticancer drug with significant clinical activity. Ann. Intern. Med. 80 (2), 249–259.
- Bronson, F.H., 1981. The regulation of luteinizing-hormone secretion by estrogen relationships among negative feedback, surge potential, and male stimulation in juvenile, Peri-pubertal, and adult female mice. Endocrinology 108 (2), 506–516.
- Brown, C., LaRocca, J., Pietruska, J., Ota, M., Anderson, L., Smith, S.D., Weston, P., Rasoulpour, T., Hixon, M.L., 2010. Subfertility caused by altered follicular development and oocyte growth in female mice lacking PKB alpha/Akt1. Biol. Reprod. 82 (2), 246–256.
- Campbell, B.K., Clinton, M., Webb, R., 2012. The role of anti-Mullerian hormone (AMH) during follicle development in a monovulatory species (sheep). Endocrinology 153 (9), 4533–4543.
- Castrillon, D.H., Miao, L., Kollipara, R., Horner, J.W., DePinho, R.A., 2003. Suppression of ovarian follicle activation in mice by the transcription factor Foxo3a. Science 301 (5630), 215–218.
- Chang, E.M., Lim, E., Yoon, S., Jeong, K., Bae, S., Lee, D.R., Yoon, T.K., Choi, Y., Lee, W.S., 2015. Cisplatin induces overactivation of the dormant primordial follicle through PTEN/AKT/FOXO3a pathway which leads to loss of ovarian reserve in mice. PLoS One 10 (12), e0144245.
- Cheung-Ong, K., Giaever, G., Nislow, C., 2013. DNA-damaging agents in cancer chemotherapy: serendipity and chemical biology. Chem. Biol. 20 (5), 648–659.
- Clark, P.A., Iranmanesh, A., Veldhuis, J.D., Rogol, A.D., 1997. Comparison of pulsatile luteinizing hormone secretion between prepubertal children and young adults: evidence for a mass/amplitude-dependent difference without gender or day/night contrasts. J. Clin. Endocrinol. Metab. 82 (9), 2950-2955.
- Cortazar, P., Justice, R., Johnson, J., Sridhara, R., Keegan, P., Pazdur, R., 2012. US Food and Drug Administration approval overview in metastatic breast cancer. J. Clin. Oncol. 30 (14), 1705–1711.
- De Bruin, M.L., Huisbrink, J., Hauptmann, M., Kuenen, M.A., Ouwens, G.M., van't Veer, M.B., Aleman, B.M., van Leeuwen, F.E., 2008. Treatment-related risk factors for premature menopause following Hodgkin lymphoma. Blood 111 (1), 101–108.
- Decanter, C., Morschhauser, F., Pigny, P., Lefebvre, C., Gallo, C., Dewailly, D., 2010. Anti-Mullerian hormone follow-up in young women treated by chemotherapy for lymphoma: preliminary results. Reprod. BioMed. Online 20 (2), 280–285.
- Ferguson, J.E., Dodwell, D.J., Seymour, A.M., Richards, M.A., Howell, A., 1993. High dose, dose-intensive chemotherapy with doxorubicin and cyclophosphamide for the treatment of advanced breast cancer. Br. J. Cancer 67 (4), 825–829.
- U.S. Food and Drug Administration, 2016. FDA grants accelerated approval to new treatment for advanced soft tissue sarcoma. from https://www.fda.gov/newsevents/ newsroom/pressannouncements/ucm525878.htm.
- Goldman, K.N., Chenette, D., Arju, R., Duncan, F.E., Keefe, D.L., Grifo, J.A., Schneider, R.J., 2017. mTORC1/2 inhibition preserves ovarian function and fertility during genotoxic chemotherapy. Proc. Natl. Acad. Sci. U. S. A. 114 (12), 3186–3191.
- Gonfloni, S., Di Tella, L., Caldarola, S., Cannata, S.M., Klinger, F.G., Di Bartolomeo, C., Mattei, M., Candi, E., De Felici, M., Melino, G., Cesareni, G., 2009. Inhibition of the c-Abl-TAp63 pathway protects mouse oocytes from chemotherapy-induced death. Nat. Med. 15 (10), 1179–1185.
- Harel, S., Ferme, C., Poirot, C., 2011. Management of fertility in patients treated for Hodgkin's lymphoma. Haematologica 96 (11), 1692–1699.
- John, G.B., Gallardo, T.D., Shirley, L.J., Castrillon, D.H., 2008. Foxo3 is a PI3K-dependent molecular switch controlling the initiation of oocyte growth. Dev. Biol. 321 (1), 197–204
- Kalich-Philosoph, L., Roness, H., Carmely, A., Fishel-Bartal, M., Ligumsky, H., Paglin, S., Wolf, I., Kanety, H., Sredni, B., Meirow, D., 2013. Cyclophosphamide triggers follicle activation and "burnout"; AS101 prevents follicle loss and preserves fertility. Sci. Transl. Med. 5 (185), 185ra162.
- Kano, M., Sosulski, A.E., Zhang, L., Saatcioglu, H.D., Wang, D., Nagykery, N., Sabatini, M.E., Gao, G., Donahoe, P.K., Pepin, D., 2017. AMH/MIS as a contraceptive that protects the ovarian reserve during chemotherapy. Proc. Natl. Acad. Sci. U. S. A. 114 (9), E1688–E1697.
- Kerr, J.B., Hutt, K.J., Michalak, E.M., Cook, M., Vandenberg, C.J., Liew, S.H., Bouillet, P., Mills, A., Scott, C.L., Findlay, J.K., Strasser, A., 2012. DNA damage-induced primordial follicle oocyte apoptosis and loss of fertility require TAp63-mediated induction of Puma and Noxa. Mol. Cell 48 (3), 343–352.

- Kim, S.Y., Cordeiro, M.H., Serna, V.A., Ebbert, K., Butler, L.M., Sinha, S., Mills, A.A., Woodruff, T.K., Kurita, T., 2013. Rescue of platinum-damaged oocytes from programmed cell death through inactivation of the p53 family signaling network. Cell Death Differ. 20 (8), 987–997.
- Kim, S.Y., Nair, D.M., Romero, M., Serna, V.A., Koleske, A.J., Woodruff, T.K., Kurita, T., 2019. Transient inhibition of p53 homologs protects ovarian function from two distinct apoptotic pathways triggered by anticancer therapies. Cell Death Differ. 26 (3), 502–515.
- Kuo, L.J., Yang, L.X., 2008. Gamma-H2AX a novel biomarker for DNA double-strand breaks. In Vivo 22 (3), 305–309.
- Kurz, E.U., Douglas, P., Lees-Miller, S.P., 2004. Doxorubicin activates ATM-dependent phosphorylation of multiple downstream targets in part through the generation of reactive oxygen species. J. Biol. Chem. 279 (51), 53272–53281.
- Levine, J.M., Whitton, J.A., Ginsberg, J.P., Green, D.M., Leisenring, W.M., Stovall, M., Robison, L.L., Armstrong, G.T., Sklar, C.A., 2018. Nonsurgical premature menopause and reproductive implications in survivors of childhood cancer: a report from the childhood Cancer survivor study. Cancer 124 (5), 1044–1052.
- Marechal, A., Zou, L., 2013. DNA damage sensing by the ATM and ATR kinases. Cold Spring Harb. Perspect. Biol. 5 (9).
- McLaughlin, M., Kelsey, T.W., Wallace, W.H.B., Anderson, R.A., Telfer, E.E., 2017. Non-growing follicle density is increased following adriamycin, bleomycin, vinblastine and dacarbazine (ABVD) chemotherapy in the adult human ovary. Hum. Reprod. 32 (1), 165–174.
- Meirow, D., Nugent, D., 2001. The effects of radiotherapy and chemotherapy on female reproduction. Hum. Reprod. Update 7 (6), 535–543.
- Minotti, G., Menna, P., Salvatorelli, E., Cairo, G., Gianni, L., 2004. Anthracyclines: molecular advances and pharmacologic developments in antitumor activity and cardiotoxicity. Pharmacol. Rev. 56 (2), 185–229.
- Molina, J.R., Barton, D.L., Loprinzi, C.L., 2005. Chemotherapy-induced ovarian failure: manifestations and management. Drug Saf. 28 (5), 401–416.
- Molnar, Z., Schneider, T., Varady, E., Fleischmann, T., 1997. ABVD chemotherapy of Hodgkin's disease. Neoplasma 44 (4), 263–265.
- Morgan, S., Anderson, R.A., Gourley, C., Wallace, W.H., Spears, N., 2012. How do chemotherapeutic agents damage the ovary? Hum. Reprod. Update 18 (5), 525–535.
- National Cancer Instititue, 2007. Doxorubicin Hydrochloride. from. https://www.cancer. gov/about-cancer/treatment/drugs/doxorubicinhydrochloride.
- Nguyen, Q.N., Zerafa, N., Liew, S.H., Morgan, F.H., Strasser, A., Scott, C.L., Findlay, J.K., Hickey, M., Hutt, K.J., 2018. Loss of PUMA protects the ovarian reserve during DNAdamaging chemotherapy and preserves fertility. Cell Death Dis. 9 (6), 618.
- Nitiss, J.L., 2009. DNA topoisomerase II and its growing repertoire of biological functions. Nat. Rev. Cancer 9 (5), 327–337.
- Pedersen, T., Peters, H., 1968. Proposal for a classification of oocytes and follicles in the mouse ovary. J. Reprod. Fertil. 17 (3), 555–557.
- Perez, G.I., Knudson, C.M., Leykin, L., Korsmeyer, S.J., Tilly, J.L., 1997. Apoptosis-associated signaling pathways are required for chemotherapy-mediated female germ cell destruction. Nat. Med. 3 (11), 1228–1232.
- Poirot, C., Dhedin, N., Brice, P., 2017. Fertility preservation before an ABVD protocol: no new evidence to support changing the recommendations. Future Oncol. 13 (7),
- Reddy, P., Shen, L., Ren, C., Boman, K., Lundin, E., Ottander, U., Lindgren, P., Liu, Y.X.,

- Sun, Q.Y., Liu, K., 2005. Activation of Akt (PKB) and suppression of FKHRL1 in mouse and rat oocytes by stem cell factor during follicular activation and development. Dev. Biol. 281 (2), 160–170.
- Reddy, P., Liu, L., Adhikari, D., Jagarlamudi, K., Rajareddy, S., Shen, Y., Du, C., Tang, W., Hamalainen, T., Peng, S.L., Lan, Z.J., Cooney, A.J., Huhtaniemi, I., Liu, K., 2008. Oocyte-specific deletion of Pten causes premature activation of the primordial follicle pool. Science 319 (5863), 611–613.
- Rossi, V., Lispi, M., Longobardi, S., Mattei, M., Di Rella, F., Salustri, A., De Felici, M., Klinger, F.G., 2017. LH prevents cisplatin-induced apoptosis in oocytes and preserves female fertility in mouse. Cell Death Differ. 24 (1), 72–82.
- Roti Roti, E.C., Salih, S.M., 2012. Dexrazoxane ameliorates doxorubicin-induced injury in mouse ovarian cells. Biol. Reprod. 86 (3), 96.
- Roti Roti, E.C., Leisman, S.K., Abbott, D.H., Salih, S.M., 2012. Acute doxorubicin insult in the mouse ovary is cell- and follicle-type dependent. PLoS One 7 (8), e42293.
- Salih, S.M., Ringelstetter, A.K., Elsarrag, M.Z., Abbott, D.H., Roti, E.C., 2015.
 Dexrazoxane abrogates acute doxorubicin toxicity in marmoset ovary. Biol. Reprod. 92 (2), 73
- Scheithauer, W., Zielinksi, C., Ludwig, H., 1985. Weekly low dose doxorubicin monotherapy in metastatic breast cancer resistant to previous hormonal and cytostatic treatment. Breast Cancer Res. Treat. 6 (1), 89–93.
- Seddon, B., Strauss, S.J., Whelan, J., Leahy, M., Woll, P.J., Cowie, F., Rothermundt, C., Wood, Z., Benson, C., Ali, N., Marples, M., Veal, G.J., Jamieson, D., Kuver, K., Tirabosco, R., Forsyth, S., Nash, S., Dehbi, H.M., Beare, S., 2017. Gemcitabine and docetaxel versus doxorubicin as first-line treatment in previously untreated advanced unresectable or metastatic soft-tissue sarcomas (GeDDiS): a randomised controlled phase 3 trial. Lancet Oncol. 18 (10), 1397–1410.
- Sonigo, C., Seroka, A., Cedrin-Durnerin, I., Sermondade, N., Sifer, C., Grynberg, M., 2016. History of ABVD alters the number of oocytes vitrified after in vitro maturation in fertility preservation candidates. Future Oncol. 12 (14), 1713–1719.
- Sonigo, C., Sermondade, N., Grynberg, M., 2017. Letter in reply to "fertility preservation before an ABVD protocol: no new evidence to support changing the recommendations". Future Oncol. 13 (7), 591–592.
- Tuppi, M., Kehrloesser, S., Coutandin, D.W., Rossi, V., Luh, L.M., Strubel, A., Hotte, K., Hoffmeister, M., Schafer, B., De Oliveira, T., Greten, F., Stelzer, E.H.K., Knapp, S., De Felici, M., Behrends, C., Klinger, F.G., Dotsch, V., 2018. Oocyte DNA damage quality control requires consecutive interplay of CHK2 and CK1 to activate p63. Nat. Struct. Mol. Biol. 25 (3), 261–269.
- Wang, Y., Liu, M., Zhang, J., Liu, Y., Kopp, M., Zheng, W., Xiao, S., 2018. Multidrug resistance protein 1 deficiency promotes doxorubicin-induced ovarian toxicity in female mice. Toxicol. Sci. 163 (1), 279–292.
- Winship, A.L., Bakai, M., Sarma, U., Liew, S.H., Hutt, K.J., 2018. Dacarbazine depletes the ovarian reserve in mice and depletion is enhanced with age. Sci. Rep. 8 (1), 6516.
- Woodward, E., Jessop, M., Glaser, A., Stark, D., 2011. Late effects in survivors of teenage and young adult cancer: does age matter? Ann. Oncol. 22 (12), 2561–2568.
- Xiao, S., Zhang, J., Liu, M., Iwahata, H., Rogers, H.B., Woodruff, T.K., 2017. Doxorubicin has dose-dependent toxicity on mouse ovarian follicle development, hormone secretion, and oocyte maturation. Toxicol. Sci. 157 (2), 320–329.
- Zhao, F., Li, R., Xiao, S., Diao, H., Viveiros, M.M., Song, X., Ye, X., 2013. Postweaning exposure to dietary zearalenone, a mycotoxin, promotes premature onset of puberty and disrupts early pregnancy events in female mice. Toxicol. Sci. 132 (2), 431–442.